PHYSICAL REVIEW B **90**, 060412(R) (2014)

# Uniaxial-pressure control of geometrical spin frustration in an Ising antiferromagnet $CoNb_2O_6$ via anisotropic deformation of the isosceles lattice

S. Kobayashi*
*Department of Materials Science and Engineering, Faculty of Engineering, Iwate University, Ueda 4-3-5, Morioka 020-8551, Japan*

S. Hosaka, H. Tamatsukuri, T. Nakajima, and S. Mitsuda
*Department of Physics, Faculty of Science, Tokyo University of Science, Shinjuku-ku, Tokyo 162-8601, Japan*

K. Prokeš and K. Kiefer
*Helmholtz-Zentrum Berlin für Materialien und Energie, Hahn-Meitner Platz 1, Berlin 14109, Germany*
(Received 10 June 2014; revised manuscript received 9 August 2014; published 26 August 2014)

We report neutron diffraction measurement results for an Ising antiferromagnet $CoNb_2O_6$ under uniaxial pressure along the geometrically frustrated isosceles-triangular-lattice direction. We find that an onset incommensurate wave number at the Néel temperature increases with pressure from 0.378 to 0.411 at 400 MPa. The observations suggest that the anisotropic deformation of the lattice by the uniaxial pressure significantly modifies the spin frustration, leading to an increase in the nearest-neighbor to next-nearest-neighbor interaction ratio from 1.33 to 1.81.

DOI: 10.1103/PhysRevB.90.060412 PACS number(s): 75.25.−j, 75.50.Ee

Geometrically frustrated triangular-lattice antiferromagnets (TLAs) have been attracting considerable interest because of their diverse phase transitions and critical phenomena [1,2] as well as the recent discovery of multiferroics properties in some TLAs [3–5]. For an ideal two-dimensional (2D) triangular lattice with a nearest-neighbor antiferromagnetic interaction, no long-range magnetic order occurs in the case of Ising spins, even at $T = 0$ K, owing to macroscopic degeneracy of the ground state, whereas a 120° structure is expected to be stabilized at $T = 0$ K for Heisenberg or *XY*-type spins. On the other hand, real TLAs usually exhibit magnetic orders at nonzero temperature, irrespective of spin type, and the phase transition is three dimensional in nature due to the stacking structure of the frustrated triangular lattice. Moreover, there exist other microscopic interactions, such as further-neighbor and dipole-dipole interactions, which reduce the degeneracy of the ground state. Nevertheless, the triangular geometrical frustration does dominate the magnetic order and diverse magnetic features have been experimentally determined in a variety of TLAs [2].

A partial releasing of the triangular geometrical frustration due to an orthorhombic distortion also has pronounced effects on magnetic ordering. This distortion splits $J$ on a triangular lattice into two inequivalent antiferromagnetic interactions, $J_1$ and $J_2$, on an isosceles-triangular lattice, as shown in Fig. 1(b). Theoretical investigation of a 2D Ising isosceles-triangular lattice revealed interesting magnetic features, which depend on the interaction ratio, $\gamma = J_1/J_2$ [6–8]. Simple long-range antiferromagnetism is achieved for $\gamma < 1.0$ of the triangular lattice, whereas for $\gamma > 1.0$ the system only shows a long-range order at $T = 0$ K, with decoupled chains along the $J_1$ direction. Above this temperature, magnetic correlations between the chains and an incommensurate magnetic order are seen. The investigation of magnets with geometrically frustrated isosceles-triangular lattices is of great importance, because such a system does not simply belong to the intermediate case between the geometrically frustrated TLA and unfrustrated magnet, but it also has the potential to exhibit unusual magnetic features absent in both magnets.

In this Rapid Communication, we report the results of neutron diffraction measurements on an isosceles-triangular-lattice Ising antiferromagnet, $CoNb_2O_6$, where uniaxial pressure was applied in the direction of the frustrated lattice in order to investigate the possible control of $\gamma$ and the resultant magnetic ordering. We observe that a change in the propagation wave vector characterizing a magnetic structure can be seen via anisotropic deformation of a frustrated isosceles-triangular lattice by a uniaxial pressure. In a columbite niobate, $CoNb_2O_6$, magnetic $Co^{2+}$ ions form quasi-one-dimensional (quasi-1D) ferromagnetic zigzag chains running along the orthorhombic $c$ axis and form an antiferromagnetic isosceles-triangular lattice in the $a$-$b$ plane, as shown in Figs. 1(a) and 1(b) [9–15]. In the zero field, the system exhibits successive magnetic phase transitions from the paramagnetic (PM) phase to the incommensurate (IC) sinusoidal magnetic phase with the temperature-dependent propagation wave vector, $\mathbf{Q}_{IC} = (0\, q\, 0)$ at $T_1 \sim 3.0$ K, and then to the noncollinear antiferromagnetic (AF) phase, with $\mathbf{Q}_{AF} = (0\ \frac{1}{2}\ 0)$ at $T_2 \sim 1.9$ K. $Co^{2+}$ spins are confined to two different easy axes in the $a$-$c$ plane with a canting angle of $\theta_0$ (=31°) from the $c$ axis, which originates from two crystallographically nonequivalent octahedral $CoO_6$ sites. Extensive neutron diffraction measurements have demonstrated interesting magnetic features reflecting the isosceles triangular geometry of Ising-like $Co^{2+}$ spins, such as rich magnetic field ($H$) versus temperature ($T$) phase diagrams [9,10,12,14,15], magnetic-structure-dependent spin correlations along the $a$ axis (originating from a partial cancellation of the exchange field) [10], and anisotropic and extremely slow domain-growth kinetics [11,13]. These features have been qualitatively explained within an isosceles-triangular-lattice Ising model with $J_1$ and $J_2$, with $\gamma$ being

*koba@iwate-u.ac.jp

 

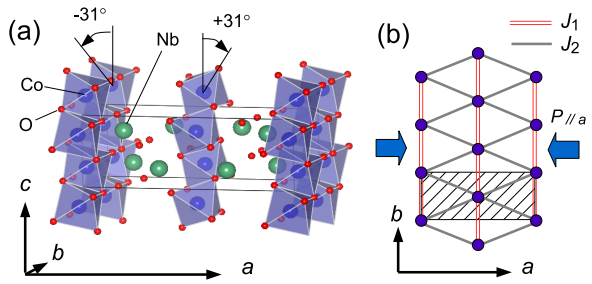


FIG. 1. (Color online) (a) Crystal structure of $CoNb_2O_6$. Two different easy axes exist in the $a$-$c$ plane with a canting angle of $\pm 31^\circ$ from the $c$ axis, which originate from the two different octahedral $CoO_6$ sites. (b) Isosceles-triangular lattice of magnetic $Co^{2+}$ ions in the $a$-$b$ plane with interchain antiferromagnetic exchange interactions, $J_1$ and $J_2$. The hatched area corresponds to a chemical unit cell and the large arrows represent the uniaxial-pressure direction, as applied in the experiment.

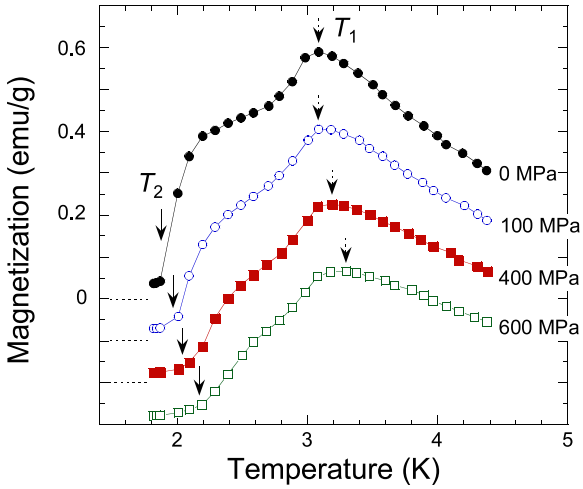


FIG. 2. (Color online) Temperature dependence of magnetization at $H = 50$ Oe on heating after zero-field cooling, taken at different uniaxial pressures along the $a$ axis. The data are shifted vertically down by 0.1 emu/g for clarity.

1.33, not far from the 1.0 of the triangular lattice. In this study, we show that the propagation wave number $q$ was successfully modified by an applied uniaxial pressure (up to 400 MPa) along the $a$ axis, leading to a change in $\gamma$ from 1.33 to 1.81.

Single crystals, grown with the flux-growth technique [16], were used. The samples were cut into plates with dimensions of $1.3 \times 2.0 \times 0.9$ mm$^3$ (weight 12.3 mg) for the magnetization measurements and with dimensions of $2.5 \times 2.2 \times 2.1$ mm$^3$ (weight 61.6 mg) for the neutron diffraction measurements. The dc magnetic measurements were performed using a commercial superconducting quantum interference device (SQUID) magnetometer (Quantum Design MPMS-XL), and a uniaxial pressure $P$ was applied along the $a$ axis, using a stick-type piston-cylinder pressure cell [17], which was inserted in the magnetometer. This pressure cell enabled us to monitor the applied pressure *in situ* using a load meter and to vary it at low temperatures, while keeping the sample inside the magnetometer. The direction of $P$ is the same as the applied field direction, and magnetization along the $a$ axis as a function of temperature was measured at a constant $P$, after varying $P$ up to a 600 MPa maximum at $T = 5$ K (above $T_1$). Neutron diffraction measurements were performed using the two-axis diffractometer, E4, installed in Helmholtz-Zentrum Berlin. A pyrolytic-graphite filter was used to eliminate second-order contamination, and incident neutrons with a wavelength of 2.44 Å were used. The same type of pressure cell as that used in the magnetic measurements was inserted in a 5 T superconducting cryomagnet, which enabled us to access the $(0\,k\,l)$ scattering plane in the reciprocal lattice under the applied uniaxial pressure. The lowest measurement temperature was ~1.7 K for both measurements.

Figure 2 shows the temperature dependence of magnetization at $H = 50$ Oe on heating after zero-field cooling, taken at different pressures along the $a$ axis. At zero applied pressure, the magnetization begins to steeply increase at $T_2 \sim 1.9$ K, followed by a peak at $T_1 \sim 3.1$ K. Here, we define $T_1$ and $T_2$ as the peak temperature of the broad maxima and the crossing point of the two magnetization extrapolation lines in the AF and IC phases, respectively. Following an increase in the uniaxial pressure, both $T_1$ and $T_2$ shift slightly toward higher temperatures, which is associated with a drastic decrease in magnetization over the entire temperature range. $T_1$ and $T_2$ increase by ~0.1 and 0.2 K, respectively, at $P = 400$ MPa.

Figure 3(a) shows the temperature dependence of the neutron diffraction profile of the $(0\,k\,0)$ reciprocal lattice

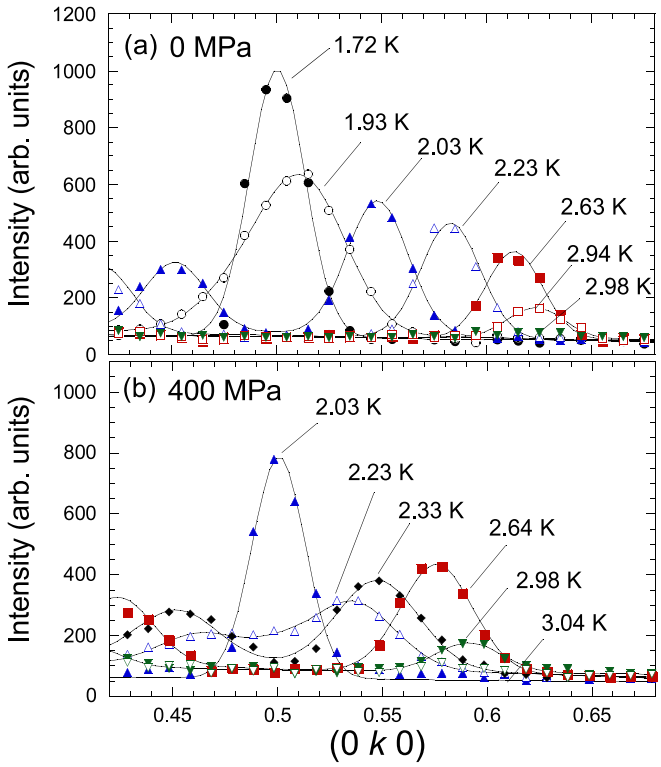


FIG. 3. (Color online) Temperature dependence of the neutron diffraction profile of the $(0\,k\,0)$ scans at (a) $P = 0$ MPa and (b) $P = 400$ MPa. In the IC phase, two magnetic reflections appear at $(0\,q\,0)$ and $(0\;1-q\;0)$. The solid lines through the data represent least-square fittings, assuming Gaussian AF and IC peaks.

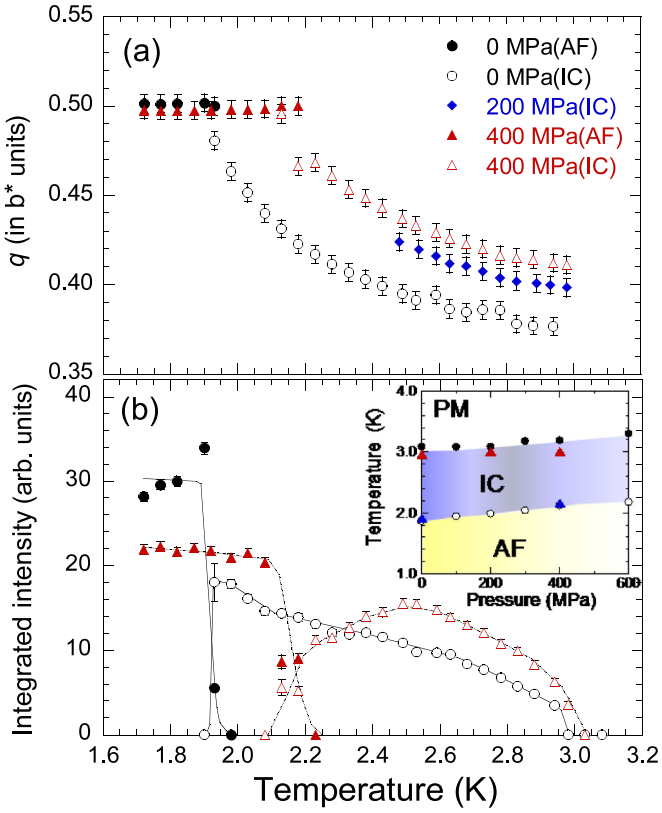


FIG. 4. (Color online) Temperature dependence of (a) the propagation wave number in the $b^*$ direction and (b) the integrated intensity of the (0 1 − $q$ 0) peak, before and after the application of uniaxial pressure. The inset in (b) shows the $P$-$T$ phase diagram obtained in this study. The circles and triangles in the inset denote magnetic phase transition temperatures, obtained by magnetization and neutron diffraction measurements, respectively. $T_2$ for the neutron diffraction data is defined as the crossing point of the two extrapolation lines of the integrated intensities of both the AF and IC phases.

scan in the $b^*$ direction at $P = 0$ MPa. With decreasing temperature (from a high temperature above $T_1$), the magnetic peaks at the incommensurate positions, such as (0 0.377 0) and (0 0.623 0), characterized by $\mathbf{Q}_{\rm IC}$ with $q = 0.377$, appear at $T_1 \sim 2.94$ K. As the temperature decreases, these IC peaks gradually shift towards the AF peak positions described by $\mathbf{Q}_{\rm AF}$, and are associated with an increase in intensity. Below $T_2 \sim 1.9$ K, both IC and AF reflections coexist. This $q$ temperature dependence is consistent with previous studies [10,14]. The variation of $q$ and the integrated intensity of the (0 1 − $q$ 0) peak is summarized in Figs. 4(a) and 4(b), respectively.

On the other hand, under a uniaxial pressure of 400 MPa along the $a$ axis, the temperature dependence is modified significantly. As the temperature decreases, IC peaks appear at $T \sim 2.98$ K, at an IC position with $q = 0.411$, as shown in Fig. 3(b), which is approximately 0.03 closer to 0.5 in comparison with the 0.377 value obtained for $P = 0$ MPa. With a further decrease in temperature, the IC peaks shift towards the AF position and the magnetic phase transition from the IC to AF phases occurs at $T \sim 2.2$ K, which is higher than the corresponding temperature for $P = 0$ MPa. The effect of uniaxial pressure on the onset of the AF ordering can be seen by comparing the diffraction profiles at $T = 2.03$ K shown in Figs. 3(a) and 3(b); while there exists a single AF peak at $k = 0.5$ at $P = 400$ MPa, only IC peaks with $q = 0.452$ are observed at $P = 0$ MPa. The temperature dependence of $q$ and the integrated intensity of the (0 1 − $q$ 0) peak after the application of uniaxial pressure is summarized in Fig. 4(a), together with the data around $T_1$ at $P = 200$ MPa. The value of $q$ at $T_1$ is 0.398 at $P = 200$ MPa, suggesting that this value monotonically increases with uniaxial pressure along the $a$ axis.

The inset of Fig. 4(b) is a $P$-$T$ magnetic phase diagram, obtained from magnetization and neutron diffraction measurements. Both magnetic phase transition temperatures, $T_1$ and $T_2$, increase slightly with uniaxial pressure and the increase in $T_2$ at $P = 400$ MPa is ∼0.2 K, which is slightly larger than that of $T_1$ for both measurements.

We now discuss the effect of uniaxial pressure on competing interactions on an isosceles-triangular lattice in $CoNb_2O_6$. Earlier extensive investigation by neutron diffraction and magnetization measurements revealed a $H$-$T$ magnetic phase diagram at no applied pressure in a magnetic field along the $a$ or $c$ axes [9,10,12,14,15]. Three-dimensional (3D) magnetic ordering below $T_1$ is achieved by interchain couplings between quasi-1D chains along the $c$ axis. This is well explained by mean-field calculations and Monte Carlo simulations for the Ising model with the ferromagnetic intrachain exchange interaction $J_0$ and antiferromagnetic interchain nearest-neighbor and next-nearest-neighbor interactions, $J_1$ and $J_2$, respectively, on the isosceles-triangular lattice in the $a$-$b$ plane, as shown in Fig. 1(b) [10]. Here, $J_0/k_{\rm B}$, estimated from $T_1$, is 0.6015 K while $J_1/k_{\rm B} = -0.0508$ K and $J_2/k_{\rm B} = -0.0381$ K, obtained from the zero-temperature critical fields of the $H_{\|c}$-$T$ magnetic phase diagram [18]. Note that the quantum fluctuation effects driven by the strong transverse magnetic field ($H \parallel b$), which were recently observed to result in the destruction of magnetic phases below $T_1$, and the appearance of a quantum paramagnetic phase, are negligible in the present case [19]. On the other hand, a value of $q$ at $T_1$ can also be estimated from mean-field calculations [10,20] and is given by

$$q = \frac{1}{\pi}\cos^{-1}(J_2/2J_1). \qquad (1)$$

The present values of exchange interactions yield $q = 0.378$ and explain the experimental value of 0.377 at $P = 0$ MPa. Under uniaxial pressure along the $a$ axis, $q$ at $T_1$ becomes greater than the value obtained at $P = 0$ MPa, with $q$ being 0.398 and 0.411 at $P = 200$ and 400 MPa, respectively. These observed $q$ at $T_1$ indicate that $\gamma$ changes from 1.33 at $P =$ 0 MPa, to 1.59 at $P = 200$ MPa, and then to 1.81 at $P =$ 400 MPa. Therefore, this suggests that the exchange interactions on the frustrated isosceles-triangular lattice are modified through anisotropic deformation by uniaxial pressure, leading to an increase in $|J_1|$ and/or a decrease in $|J_2|$ within the isosceles-triangular-lattice Ising model.

As revealed in Fig. 4, a slight increase in $T_1$ with uniaxial pressure, i.e., an approximately 0.05 K increase at 400 MPa, was observed. Within the mean-field approximation, $T_1$ is

related to $J_0$, $J_1$, and $J_2$, and is expressed, using $\gamma$, as

$$k_B T_1 = \left\{ 2J_0 + 2|J_1| \left( \frac{1}{2\gamma^2} + 1 \right) \right\} S^2, \quad (2)$$

where $S = \frac{3}{2}$ [10]. The observed increase in $T_1$ suggests that $J_0$ and/or $|J_1|$ increase with uniaxial pressure. In this system, the intrachain interaction along the $c$ axis, $J_0$, results from the superexchange interactions based on the 90° $Co^{2+}$-$O^{2-}$-$Co^{2+}$ bond angle. On the other hand, the interchain exchange interactions between the magnetic $Co^{2+}$ ions are generally achieved by complicated exchange paths through the $O^{2-}$ and $Nb^{5+}$ ions. There are at least four and six bond lengths for $J_1$ and $J_2$, respectively. Uniaxial pressure changes the atomic distances and these interchain interactions may vary in a different way with each other, because of the complexity of the exchange paths. According to high-pressure x-ray diffraction measurements at room temperature for columbite compounds, the distance between neighboring cations along the $a$ or $b$ axis ($Co^{2+}$-$Nb^{5+}$ distance in our case) is more variable by pressure than that along the $c$ axis ($Co^{2+}$-$Co^{2+}$ distance) [21]. Assuming that uniaxial pressure along the $a$ axis mainly modifies atomic distances along the $a$ and $b$ axes, and that the observed increase of $T_1$ is attributable only to a change in $J_1$ and $J_2$ in $CoNb_2O_6$, $J_1/k_B$ would change from $-0.0508$ to $-0.0652$ K with $P = 400$ MPa, which is approximately a 28% increase. This also suggests a change in $J_2$ from $-0.0382$ to $-0.0360$ K at $P = 400$ MPa (a decrease of approximately 6%). Detailed x-ray diffraction measurements under uniaxial pressure may clarify the exchange mechanism in $CoNb_2O_6$.

In this study, we have shown that uniaxial pressure up to 400 MPa results in a significant change in the exchange interaction ratio on the geometrically frustrated isosceles-triangular lattice in $CoNb_2O_6$, as evidenced by a change in the temperature dependence of its magnetic propagation wave number. Extensive studies have reported pressure control of geometrical spin frustration in TLAs. For instance, under hydrostatic pressures of up to 5 GPa, enhancement of triangular spin frustration, associated with a reduction in the ordered Mn moments, was observed for $RMnO_3$, with $R$ = Y [22,23] and Lu [24] with a 120° structure, whereas stabilization of ordered phases was observed in $CsNiCl_3$ [25]. In the case of $CuFeO_2$, hydrostatic pressure up to 7.9 GPa suppresses spontaneous structural distortion due to temperature-dependent exchange interactions, leading to the disappearance of the lowest-temperature commensurate magnetic phase, as well as the appearance of interesting pressure-induced phase transitions [26,27]. These studies reveal the significant effect of hydrostatic pressure as regards the modification of exchange interactions in TLAs, however, the controllability of the exchange interaction ratio $\gamma$ is limited because of the isotropic nature of the hydrostatic pressure. In parallel to these studies, some attempts to anisotropically control the triangular geometry of the spins using uniaxial pressure have been made for single TLA crystals such as $RbMnBr_3$ [28] and $CuFeO_2$ [17,29–31]. By changing the uniaxial-pressure direction with respect to the crystal axis, it may be possible to increase, decrease, and tune the ratio of the exchange interactions on a triangular lattice in a controllable way. For $RbMnBr_3$, a significant decrease in the critical field from the incommensurate to commensurate phases was observed through antiferromagnetic resonance measurements under uniaxial pressure along the direction perpendicular to the hexagonal lattice, and a modification of the periodic variation of the exchange interactions in the lattice was inferred [28]. On the other hand, in the case of $CuFeO_2$, an increase in the Néel temperature from the paramagnetic to the incommensurate state, by ∼1.3 K, as well as a change in the volume fraction of the spin-lattice-coupled domains were observed under a uniaxial pressure up to 100 MPa along the direction of the triangular lattice [17,29–31]. These results indicate that the uniaxial pressure breaks the equilateral symmetry of the triangular lattice above the original transition temperature, and partially relieves geometrical spin frustration of a triangular lattice. Unlike in the case of a hydrostatic pressure, the spin frustration can be controlled in $CuFeO_2$ by a uniaxial pressure, however, a change in the associated magnetic propagation vector was not confirmed for pressures up to 100 MPa. Despite extensive studies under uniaxial pressure, direct observations that reveal controllability of the exchange interaction ratio still need to be reported. In the present investigation, samples with an optimal size and shape for uniaxial-pressure studies were used, and a maximum uniaxial pressure of 400 MPa was successfully attained using the same pressure cell as that of our previous studies [17,29–31]. This higher uniaxial pressure may enable us to clearly observe a change in the propagation wave vector in $CoNb_2O_6$, which indicates an increase in the nearest-neighbor to next-nearest-neighbor interaction ratio $\gamma$ from 1.33 to 1.81. Further investigation into the possible control of the $\gamma$ of a triangular lattice toward 1.0 by application of uniaxial pressure in directions such as along the $b$ axis is now in progress.

This work was supported by a Grant-in-Aid for Scientific Research (C) (Grant No. 23540424) from JSPS, Japan. The crystal structure figure was drawn using the VESTA software [32].

[1] H. T. Diep, *Frustrated Spin Systems* (World Scientific, Singapore, 2004).
[2] M. F. Collins and O. A. Petrenko, Can. J. Phys. **75**, 605 (1997).
[3] T. Kimura, J. C. Lashley, and A. P. Ramirez, Phys. Rev. B **73**, 220401(R) (2006).
[4] T. Nakajima, S. Mitsuda, S. Kanetsuki, K. Tanaka, K. Fujii, N. Terada, M. Soda, M. Matsuura, and K. Hirota, Phys. Rev. B **77**, 052401 (2008).
[5] S. Seki, Y. Onose, and Y. Tokura, Phys. Rev. Lett. **101**, 067204 (2008).
[6] J. Stephenson, J. Math. Phys. **11**, 420 (1970).
[7] J. Stephenson, Can. J. Phys. **48**, 2118 (1970).
[8] J. Doczi-Reger and P. C. Hemmer, Physica A **108**, 531 (1981).
[9] T. Hanawa, K. Shinkawa, M. Ishikawa, K. Miyatani, K. Saito, and K. Kohn, J. Phys. Soc. Jpn. **63**, 2706 (1994).
[10] S. Kobayashi, S. Mitsuda, M. Ishikawa, K. Miyatani, and K. Kohn, Phys. Rev. B **60**, 3331 (1999).

[11] S. Kobayashi, S. Mitsuda, T. Jogetsu, J. Miyamoto, H. Katagiri, and K. Kohn, Phys. Rev. B **60**, R9908 (1999).

[12] S. Kobayashi, S. Mitsuda, and K. Prokes, Phys. Rev. B **63**, 024415 (2000).

[13] S. Kobayashi, H. Okano, T. Jogetsu, J. Miyamoto, and S. Mitsuda, Phys. Rev. B **69**, 144430 (2004).

[14] C. Heid, H. Weitzel, P. Burlet, M. Bonnet, W. Gonschorek, T. Vogt, J. Norwig, and H. Fuess, J. Magn. Magn. Mater. **151**, 123 (1995).

[15] H. Weitzel, H. Ehrenberg, C. Heid, H. Fuess, and P. Burlet, Phys. Rev. B **62**, 12146 (2000).

[16] B. M. Wanklyn, B. J. Garrard, and G. Garton, Mater. Res. Bull. **11**, 1497 (1976).

[17] T. Nakajima, S. Mitsuda, K. Takahashi, K. Yoshitomi, K. Masuda, C. Kaneko, Y. Honma, S. Kobayashi, H. Kitazawa, M. Kosaka, N. Aso, Y. Uwatoko, N. Terada, S. Wakimoto, M. Takeda, and K. Kakurai, J. Phys. Soc. Jpn. **81**, 094710 (2012).

[18] In the present study, we redefined the $J_2 \cos 2\theta_0$ of our previous study [10] as $J_2$ for simplicity. Here, the term $\cos 2\theta_0$ originates from the two different easy axes along which the Co spins align.

[19] R. Coldea, D. A. Tennant, E. M. Wheeler, E. Wawrzynska, D. Prabhakaran, M. Telling, K. Habicht, P. Smeibidl, and K. Kiefer, Science **327**, 177 (2010).

[20] P. Bak and J. von Boehm, Phys. Rev. B **21**, 5297 (1980).

[21] S. C. Tarantino, M. Zema, and T. B. Ballaran, Phys. Chem. Miner. **37**, 769 (2010).

[22] D. P. Kozlenko, S. E. Kichanov, S. Lee, J.-G. Park, V. P. Glazkov, and B. N. Savenko, JETP Lett. **82**, 193 (2005).

[23] T. Lancaster, S. J. Blundell, D. Andreica, M. Janoschek, B. Roessli, S. N. Gvasaliya, K. Conder, E. Pomjakushina, M. L. Brooks, P. J. Baker, D. Prabhakaran, W. Hayes, and F. L. Pratt, Phys. Rev. Lett. **98**, 197203 (2007).

[24] D. P. Kozlenko, S. E. Kichanov, S. Lee, J.-G. Park, V. P. Glazkov, and B. N. Savenko, JETP Lett. **83**, 346 (2006).

[25] M. Ito, T. Asano, T. Kawae, Y. Ajiro, and K. Takeda, J. Phys.: Condens. Matter **15**, L681 (2003).

[26] N. Terada, T. Osakabe, and H. Kitazawa, Phys. Rev. B **83**, 020403(R) (2011).

[27] N. Terada, D. D. Khalyavin, P. Manuel, T. Osakabe, P. G. Radaelli, and H. Kitazawa, Phys. Rev. B **89**, 220403(R) (2014).

[28] L. A. Prozorova, S. S. Sosin, and S. V. Petrov, JETP Lett. **77**, 680 (2003).

[29] T. Nakajima, S. Mitsuda, T. Haku, K. Shibata, K. Yoshitomi, Y. Noda, N. Aso, Y. Uwatoko, and N. Terada, J. Phys. Soc. Jpn. **80**, 014714 (2011).

[30] T. Nakajima, S. Mitsuda, T. Nakamura, H. Ishii, T. Haku, Y. Honma, M. Kosaka, N. Aso, and Y. Uwatoko, Phys. Rev. B **83**, 220101(R) (2011).

[31] S. Mitsuda, K. Yoshitomi, T. Nakajima, C. Kaneko, H. Yamazaki, M. Kosaka, N. Aso, Y. Uwatoko, Y. Noda, M. Matsuura, N. Terada, S. Wakimoto, M. Takeda, and K. Kakurai, J. Phys.: Conf. Ser. **340**, 012062 (2012).

[32] K. Momma and F. Izumi, J. Appl. Crystallogr. **44**, 1272 (2011).